

# Theory of Excitons in Insulating Cu-Oxide Plane

F. C. Zhang, K. K. Ng

*Department of Physics, University of Cincinnati, Cincinnati, Ohio 45221*

We use a local model to study the formation and the structure of the low energy charge transfer excitations in the insulating Cu-O<sub>2</sub> plane. The elementary excitation is a bound exciton of spin singlet, consisting of a Cu<sup>+</sup> and a neighboring spin singlet of Cu-O holes. The exciton can move through the lattice freely without disturbing the antiferromagnetic spin background, in contrast to the single hole motion. There are four eigen-modes of excitons with different symmetry. The *p*-wave-like exciton has a large dispersion width. The *s*-wave-like exciton mixes with *p*-state at finite momentum, and its dipole transition intensity is strongly anisotropic. The model is in excellent agreement with the electron energy loss spectra in the insulating Sr<sub>2</sub>CuO<sub>2</sub>Cl<sub>2</sub>.

PACS numbers: 71.35.Cc, 74.72.Jt

## I. INTRODUCTION

There have been extensive efforts in recent several years on the electronic structure in the layered Cu-oxides, in the hope to reveal the mechanism for the high  $T_c$  superconductivity. It is now well established that the low energy physics of the undoped cuprates is well described by the spin-1/2 Heisenberg model in a square lattice, leading to an antiferromagnetic insulator. Two-dimensional  $t - J$  model has been proposed and argued to describe the low energy physics for the cuprates [1,2], and it seems the model explains many unusual properties of the high  $T_c$  materials.

In this paper we present a theory for the lower energy charge transfer excitations in the insulating Cu-oxide plane. Our work was motivated by the angle-resolved electron energy loss spectra (EELS) in the insulating Sr<sub>2</sub>CuO<sub>2</sub>Cl<sub>2</sub>, where the optical allowed transition shows a large energy dispersion width 1.5 eV, and the optical forbidden transition was observed to be strongly anisotropic [3].

We use a local model to analyze the formation and the structure of the charge transfer excitation between Cu-3 $d_{x^2-y^2}$  and O-2 $p\sigma$  in the Cu-oxide planes. The elementary charge transfer excitation is a bound exciton of spin singlet, consisting of a Cu<sup>+</sup> (quasi-particle) and a neighboring spin singlet of Cu-O holes. The exciton can move through the lattice freely without disturbing the antiferromagnetic (AF) spin background, in contrast to the single hole motion. There are four exciton modes related to the four-fold rotation symmetry in the lattice, whose hopping matrices determine the dynamics and the symmetry of the charge transfer excitations. The *p*-wave like exciton has a large energy dispersion width. The *s*-wave-like exciton mixes with the *p*-state at finite  $\mathbf{k}$ , and its optical transition intensity is strongly anisotropic. The model is in excellent agreement with the recent electron energy loss spectra in the insulating Sr<sub>2</sub>CuO<sub>2</sub>Cl<sub>2</sub>. The theory also predicts a lower energy optical forbidden mode, which should be observable in luminescence experiment [4]. Since the mass of the particle-hole pair is heavier than the particle or the hole in a usual semicon-

ductor or in other band-like insulator materials [5], the anomalous behavior of the dispersion widths between the single hole and the exciton in cuprates provides further evidence for the strong correlation in these compounds. A part of the results in this paper was briefly reported in a joined article with the EELS experiments [3]. The paper is organized as follows. In section II, we examine the formation and the structure of small excitons in the insulating cuprates. The dynamics of the excitons is derived in section III. The exciton eigen-modes and the relevance to the charge transfer gap and to the EELS are described in section IV. Several remarks and discussions are made in section V.

## II. STRUCTURE OF SMALL EXCITONS

We consider a Cu-oxide plane, where the vacuum is the filled shell states of Cu<sup>+</sup> and O<sup>2-</sup>. In the undoped case, there is one hole in average in each unit cell of CuO<sub>2</sub>, and the hole primarily resides on the Cu site and is of  $d_{x^2-y^2}$  symmetry. Because of the strong on-site Coulomb repulsion between the Cu holes, the ground state is a spin-1/2 antiferromagnet of Cu<sup>2+</sup>. To study the low energy charge excitations of a particle-hole pair, we shall focus on the transition from the Cu-3 $d_{x^2-y^2}$  to O-2 $p\sigma$  states. This transition is of particular interest due to the relatively small atomic energy difference and due to the large orbital overlap between the two states hence the strong intensity in experiments. The measured optical gap [6] is related to this transition.

Let us start with a local pair of particle and hole and examine the formation and the structure of the exciton. As illustrated in Fig. 1, the quasi-particle is at a vacant Cu-site (Cu<sup>+</sup>), and the quasi-hole is at the O-site. There are two important physical effects for the pair. The first is the Coulomb attraction between the particle and the hole, which should be considerably large in the insulating compounds where the screening effect is weak. It is this attraction to bind the pair to form an exciton. For simplicity we shall assume the attractive potential to be short-ranged, which is  $-E_c < 0$  when the particle

and hole are nearest neighbors (n.n.), and is zero otherwise. We expect that the more realistic potentials will not change the basic physics as long as the n.n. attraction dominates. The second is the strong Cu-O hybridization which binds a hole on each square of O-atoms to the central Cu-hole to form a spin singlet [2]. Let us denote this binding energy to be  $E_s$ . As a compromise of the above two effects, we expect a spin singlet with more weight of the O-hole on the site near the  $\text{Cu}^+$ . We can make the above argument more quantitatively using variation approach. Let the O-hole state be

$$\Phi = \alpha P_{-\hat{x}/2} + \beta (-P_{\hat{x}/2} + P_{\hat{y}/2} - P_{-\hat{y}/2}), \quad (1)$$

where  $P$  is the atomic O-hole orbital, whose sub-index denotes the atomic position relative to their central Cu-hole (lattice constant=1), and  $P_{-\hat{x}/2}$  is the one close to the  $\text{Cu}^+$ . The total binding energy of the exciton,  $E_b$ , takes maximum when  $\alpha^2 = (1 + 1/\sqrt{1+3c})/2$ , with  $c = E_s^2/(2E_c - E_s)^2$ . Typically,  $\alpha^2 = 0.5$  or  $0.75$  for  $E_c/E_s=0.5$  or  $1$ . From the above analysis we see that the exciton in cuprates is a complex object, consisting of a  $\text{Cu}^+$  and a nearby Cu-O singlet. The spin triplet exciton energy has a binding energy of  $E_c$ , smaller than the binding energy  $E_b$  of the spin singlet exciton, and will not be considered in this paper.

The parameters  $E_c$  and  $E_s$  in cuprates should be within certain regions so that the system is stable against the excitonic excitations. Let  $\epsilon_p$  be the atomic energy difference between the Cu- and O-hole states, the stability condition in the local limit is  $E_b < \epsilon_p$ . If we further consider an extra hole (primarily residing on O-site) in the half-filled insulating Cu-oxides, the model system should be stable against excitonic excitation (one of the Cu-hole moves to the oxygen). This implies  $2E_b < \epsilon_p + E_s$ . Our discussion in this paper will be limited to the above physical parameter region.

There are four spin singlet exciton states for a fixed quasi-particle at  $\mathbf{R}$ , denoted by  $\tau(\mathbf{R})$ , where  $\tau$  is the coordinator of the Cu-site in the singlet relative to  $\mathbf{R}$ .  $\tau = \hat{x}, -\hat{x}, \hat{y}$ , and  $-\hat{y}$ . These will be briefly denoted by  $x, \bar{x}, y$ , and  $\bar{y}$  respectively (see Fig. 1).

### III. DYNAMICS OF EXCITONS

The exciton can move through the lattice due to the n.n. Cu-O hopping  $t_{pd}$  and the O-O direct hopping  $t_{pp}$ . The most important feature of the exciton dynamics is that the exciton motion does not disturb the AF spin background. This is because each exciton involves two neighboring Cu-sites, both are spinless. As far as spins are concerned, the spin singlet exciton is similar to a pair of bound n.n. holes, whose motion does not disturb the AF spin background. This property should be compared with the single hole dynamics in Cu-oxide, where the AF spin background is strongly disturbed, and the hole dispersion is given by the Cu-Cu spin exchange interaction

$J$  instead of the hole hopping integral  $t$ , as shown theoretically for the  $t-J$  model [7] and observed in the recent angle-resolved photoemission experiments [4]

We now study the exciton motion quantitatively. A general hopping process of the exciton in the coordinator space may be represented by  $\tau(\mathbf{R}) \rightarrow \tau'(\mathbf{R}')$  with the hopping integral  $t_{\tau\tau'}(\mathbf{R}-\mathbf{R}')$ . Because the AF spin background is unchanged [8], the exciton motion is equivalent to that for a free particle. Let  $|GS\rangle$  be the AF ground state, and  $\gamma_{\tau}^{\dagger}(\mathbf{R})$  is an operator to create an exciton  $\tau(\mathbf{R})$  in the ground state, so that  $\gamma_{\tau}^{\dagger}(\mathbf{R})|GS\rangle$  is the state of exciton  $\tau(\mathbf{R})$  in an otherwise AF spin background. The exciton hopping is described by an effective Hamiltonian  $H_{eff}$ , which acts on the Hilbert space of the single exciton states,

$$H_{eff}\gamma_{\tau}^{\dagger}(\mathbf{R})|GS\rangle = \sum_{\mathbf{R}',\tau'} t_{\tau\tau'}(\mathbf{R}-\mathbf{R}')\gamma_{\tau'}^{\dagger}(\mathbf{R}')|GS\rangle. \quad (2)$$

It follows that

$$H_{eff} = \sum_{\mathbf{k}} \gamma^{\dagger}(\mathbf{k})T(\mathbf{k})\gamma(\mathbf{k}), \quad (3)$$

with  $\gamma^{\dagger}(\mathbf{k}) = (\gamma_x^{\dagger}, \gamma_{\bar{x}}^{\dagger}, \gamma_y^{\dagger}, \gamma_{\bar{y}}^{\dagger})$ .  $T(\mathbf{k})$  is a 4 by 4 matrix, which determines the exciton dynamics, and  $T_{\tau\tau'}(\mathbf{k}) = \sum_{\mathbf{r}} t_{\tau\tau'}(\mathbf{r})e^{i\mathbf{k}\cdot\mathbf{r}}/N$ , with  $N$  the number of Cu-sites. Note that  $\mathbf{k}$  is in the whole first Brillouin zone although there are two sub-lattices in the ground state. The matrix is hermitian,  $T_{\tau\tau'}(\mathbf{k}) = T_{\tau'\tau}^*(\mathbf{k})$ . Because  $t_{\tau\tau'}(\mathbf{r})$  is real, we have  $T_{\tau\tau'}(\mathbf{k}) = T_{\tau'\tau}^*(-\mathbf{k})$ . The Cu-O plane has certain symmetries. Taking into account of the Cu and O-hole orbital symmetries, we have  $T_{\tau\tau'}(\mathbf{k}) = T_{\bar{\tau}\bar{\tau}'}(-\mathbf{k})$  from the parity invariance,  $T_{x\bar{y}}(k_x, k_y) = -T_{x\bar{y}}(k_x, -k_y)$  from the inversion symmetry with respect to the x-axis, and  $T_{x\bar{x}}(k_x, k_y) = T_{y\bar{y}}(-k_y, k_x)$  due to the four-fold rotational invariance.

To pursue the theory further, we estimate the hopping integral  $t_{\tau\tau'}(\mathbf{r})$  within the atomic limit and treat  $t_{pd}$  and  $t_{pp}$  perturbatively. We shall consider the limit  $\alpha = 1$  in Eq.(1) for simplicity and for the purpose of illustration. Up to the third order in perturbation in  $t_{pd}$  or  $t_{pp}$ , there are only four non-zero independent integrals:

$$\begin{aligned} t_1 &\equiv t_{xy}(0) = \frac{1}{2}(t_{pp} - t_{pd}^2/\epsilon_p), \\ t_2 &\equiv t_{xy}(\hat{x}) = t_{pp}t_{pd}^2/(2\epsilon_p E_c), \\ t_3 &\equiv -t_{x\bar{x}}(\hat{x}) = t_{pd}^2[\epsilon_p^{-1} - (\epsilon_p + U_{pp})^{-1}], \\ t_4 &\equiv t_{x\bar{x}}(0) = t_{pd}^2/(2\epsilon_p). \end{aligned} \quad (4)$$

A diagrammatic illustration for these hopping processes are shown in Fig. 2. In Eq. (4),  $U_{pp}$  is the on-site O-hole Coulomb repulsion. We have kept the third order term,  $t_2$ , because  $E_c$  is small compared to  $\epsilon_p$ . From Eq. (4),  $t_3 > t_4$ . Since  $t_{pp} > 0$  for the O-oxygen hole hopping,  $t_2, t_3$ , and  $t_4$  are all positive. Using these  $t$ 's and the symmetries discussed above, we obtain

$$T(\mathbf{k}) = \begin{pmatrix} 0 & a(k_x) & b(\mathbf{k}) & \bar{b}(\mathbf{k}) \\ a^*(k_x) & 0 & \bar{b}^*(\mathbf{k}) & b^*(\mathbf{k}) \\ b^*(\mathbf{k}) & \bar{b}(\mathbf{k}) & 0 & a(k_y) \\ \bar{b}^*(\mathbf{k}) & b(\mathbf{k}) & a^*(k_y) & 0 \end{pmatrix}, \quad (5)$$

where  $\bar{b}(k_x, k_y) = -b(k_x, -k_y)$ , and

$$\begin{aligned} a(k_x) &= t_4 - t_3 e^{ik_x}, \\ b(\mathbf{k}) &= t_1 + t_2 (e^{ik_x} + e^{-ik_y}). \end{aligned} \quad (6)$$

#### IV. EXCITON EIGEN-MODES

$H_{eff}$  can be diagonalized to obtain the exciton solutions. For  $\mathbf{k}$  along [11] direction, the analytical solutions are particularly simple and are listed in Table I. At  $\mathbf{k}=0$ , the four exciton eigenstates have well defined local symmetry [9], describing the uniformly moving molecular states. They are illustrated in Fig. 3. The  $s$ -wave and  $d$ -wave states are given by

$$\begin{aligned} |s\rangle &= \left(-\frac{1}{2}, \frac{1}{2}, -\frac{1}{2}, \frac{1}{2}\right), \\ |d\rangle &= \left(-\frac{1}{2}, \frac{1}{2}, \frac{1}{2}, -\frac{1}{2}\right), \end{aligned} \quad (7)$$

where the four components represent the amplitudes of the excitons  $\gamma_x, \gamma_{\bar{x}}, \gamma_y, \gamma_{\bar{y}}$  respectively. The energies for  $s$ - and  $d$ -states are  $2b_0 - a_0$ , and  $-2b_0 - a_0$  respectively, where  $a_0$  and  $b_0$  are their values at  $\mathbf{k} = 0$ , and  $a_0 = t_4 - t_3 > 0$ ,  $b_0 = t_1 + t_2$ . The two  $p$ -wave states are degenerate and the energy is  $-a_0$ . In the parameter region  $-b_0 < a_0 < b_0$  and  $b_0 > 0$  (suitable for Cu-oxide, see Fig. 4 caption), the  $s$ -wave state has the highest energy [10]. The optical experiment measures the dipole active mode at  $k=0$ . Because of the  $d$ -symmetry of the Cu-hole, both the  $s$ - and  $d$ -wave modes are optically forbidden. The  $p$ -wave modes are optically active, and the charge transfer gap is given by

$$\Delta = \epsilon_p - E_b - a_0. \quad (8)$$

For finite  $k$  along an arbitrary direction  $\hat{k}$ , the eigenstate of the exciton is a linear combination of the molecular states. We shall denote the four exciton modes by  $P_1, P_2, S$ , and  $D$ , according to their symmetries  $p_1, p_2, s$ ,  $d_{x^2-y^2}$  in the limit  $k \rightarrow 0$ . For the two  $p$ -states, we define a dipole active mode  $|p_1\rangle$  and a dipole inactive mode  $|p_2\rangle$  as

$$\begin{aligned} |p_1\rangle &= (-k_x, -k_x, k_y, k_y)/(\sqrt{2}k), \\ |p_2\rangle &= (k_y, k_y, k_x, k_x)/(\sqrt{2}k). \end{aligned} \quad (9)$$

The exciton dispersions are plotted in Fig. 4. The parameters are chosen [11] to fit the measured EELS [3]. The dispersions are anisotropic. The  $E - \mathbf{k}$  relation of the  $P_1$  mode is monotonic, and the energy is peaked at

$\mathbf{k} = (\pi, \pi)$ . The dispersion width is  $2t_3 \sim 2t_{pd}^2/\epsilon_p$ , which is a large energy scale, order of the hole hopping integral in cuprates, but much larger than the dispersion width of the single hole motion in the AF background which is  $\sim J$  [7]. This result is consistent with the EELS [3]. The dispersion along [10] direction is much flatter, also consistent with the EELS. As we can see from Fig. 4, the lowest energy mode is the  $D$ -mode. This is in agreement with the weak coupling method of Littlewood, Varma, and Schmitt-Rink [12].

In the EELS, an incident electron is inelastically scattered to create a pair of electron-hole with energy and crystal momentum  $(\omega, \mathbf{k})$ . The EELS directly measures  $\text{Im}[-1/\epsilon(\mathbf{k}, \omega)]$ , with  $\epsilon(\mathbf{k}, \omega)$  the dielectric function, hence probes the dispersion and the symmetry of the charge transfer excitation [13]. For an exciton, the intensity in the imaginary part of  $\epsilon(\mathbf{k}, \omega)$  around a pole is,

$$I = \text{const} * k^{-2} |\langle \Psi_{ex} | e^{i\mathbf{k}\cdot\mathbf{r}} | GS \rangle|^2, \quad (10)$$

where  $\Psi_{ex}$  is the exciton state. For small  $\mathbf{k}$ , the most dipole active excitations in the EELS can be identified to be the  $P_1$  mode. The dispersion obtained from the EELS [3] compares well with the theory. As  $k$  increases, the  $S$ - and  $D$ -mode excitons gradually become EELS active because of the mixing of the  $|p_1\rangle$  molecular state and because of the quadrupole contribution. It is difficult to make a quantitative comparison between the dipole and quadrupole contributions in the  $S$ - or  $D$ -mode. However, if the radius of the Cu-3d state is much smaller than the lattice constant, the dipole contribution is more important. We expect this to be the case in cuprates. Within the dipole approximation, we have

$$I = I_0 |\langle \Psi_{ex} | p_1 \rangle|^2. \quad (11)$$

where  $I_0$  is the dipole active intensity of  $P_1$ -mode at  $\mathbf{k}=0$ . Note the total dipole active intensity of the four modes is conserved to be  $I_0$ . In Fig. 5, we show the calculated intensity  $I$  of the excitons in Eq. (11) as functions of  $\mathbf{k}$ . Along [10] direction, as  $k$  increases, the intensity of the  $S$ -mode increases rapidly, while the intensity of the  $P_1$ -mode decreases. The intensity along [11] is quite flat for the  $P_1$ -mode and remains to be zero for the  $S$ -mode. This anisotropy is due to the symmetry of the exciton states. The  $S$ -mode eigenstate along [11] contains only  $s$  and  $p_2$  states, both are dipole inactive. Furthermore, the transition matrix from the quadrupole contribution is proportional to  $\langle \Psi_{ex} | e^{i\mathbf{k}\cdot\mathbf{r}} | GS \rangle$ , which is  $(k_x^2 - k_y^2)$  for the  $s$ -state [14]. Therefore, the intensity for the  $S$ -mode along [11] vanishes up to the quadrupole order. These features are in excellent agreement with the EELS experiment [3], where an optical forbidden transition was observed along [10] but not along [11] direction, and the intensity of the optical active transition along [10] direction is observed in the experiment to decrease as  $\mathbf{k}$  increase.

The  $D$ -mode exciton, expected from the theory, is another optical forbidden state. The current EELS has not revealed this mode, probably due to the limit of the experiment resolution. Further spectroscopy measurements are needed to verify this  $d$ -wave-like state. This mode can be active in the phonon-assisted optical process, and should be observable in the luminescence experiment. A recent optical absorption measurement indicates a very weak absorption state at about 0.5 eV in the undoped cuprates [14]. The  $d$ -symmetry state is an alternative to the magnon state or crystal field exciton proposed earlier for this weak absorption where the phonons could be involved.

## V. DISCUSSIONS

In this paper we discussed small excitons in the insulating Cu-oxide planes. These are the charge transfer excitations, which are separated from the lower energy excitations by an energy order of  $\epsilon_p$ . The lower energy excitations are the magnons described by spin -1/2 Heisenberg model at half-filled. In the doped case, the lower energy charge excitations are given by the hole motion in the AF spin background described by the 2-dimensional  $t - J$  model.

We have used a local model to describe the excitons in Cu-oxide planes. If we include the individual kinetic energies of the quasi-particle and the quasi-hole, the excitons should have spatial extensions. The size of the exciton is determined by the balance of the kinetic energies and the Coulomb attraction  $E_c$ . This spatial extension will lower the exciton energy. The exciton motion will be more complicated, and will contain an incoherent part disturbing the AF background. The large dispersion width observed in the EELS may be viewed as an experimental indication that the spatial extension of the exciton does not play an important role and the small exciton proposed here may be a good approximation.

We have so far not considered the electron-hole (e-h) continuum, which starts at energy  $\Delta_{e-h} = \epsilon_p - E_s + E_{Kin}$ , where  $E_{Kin} < 0$  is the lowest kinetic energy of the independent  $\text{Cu}^+$  and the formal  $\text{Cu}^{3+}$ . For the cuprates,  $|E_{Kin}| \sim 1 - 2$  eV. We expect the e-h continuum to start above the  $\mathbf{k}=0$   $p_1$  mode, and the exciton spectra extend into the e-h continuum due to the large spectral dispersion. The states within the continuum region will then be damped, but can exist as resonant states contributing to the EELS. Since the contributions to the EELS from the e-h continuum have much less  $\mathbf{k}$ -dependence, the excitons become the dominant source of the  $\mathbf{k}$ -dependent spectra in the EELS.

Our model applies to the insulating phase. In the metallic phase the Coulomb attraction between the quasi-hole and quasi-particle is substantially reduced due to the metallic screening, and is too weak to bind a pair.

In conclusion, we have studied a local exciton model

for the insulating Cu-oxides. The exciton moves through the lattice almost freely in the AF spin background. The model is in excellent agreement with the recent EELS in the insulating  $\text{Sr}_2\text{CuO}_2\text{Cl}_2$ .

## VI. ACKNOWLEDGMENT

We wish to thank Y.Y. Wang and M.V. Klein for numerous discussions on both experimental and theoretical aspects related to the present work. We would also like to thank T.M. Rice and C.M. Varma useful discussions.

- 
- [1] P.W. Anderson, *Science* **235**, 1196 (1987).
  - [2] F.C. Zhang and T.M. Rice, *Phys. Rev. B* **37**, 3759 (1988).
  - [3] Y.Y. Wang, F.C. Zhang, V.P. Dravid, K.K. Ng, M.V. Klein, S.E. Schnatterly, and L.L. Miller, *Phys. Rev. Lett.* **77**, 1809 (1996). *Phys. Rev. Lett.* **75**, 2546 (1995).
  - [4] B.O. Wells, Z.X. Shen, A. Matsuura, D.M. King, M. Kastner, M. Greven, and R.J. Birgeneau, *Phys. Rev. Lett.* **74**, 964 (1995).
  - [5] D.C. Mattis and J.P. Gallinar, *Phys. Rev. Lett.* **53**, 1391 (1984).
  - [6] S. Uchida, T. Ido, H. Takagi, T. Arima, Y. Tokura, and S. Tajima, *Phys. Rev. B* **43**, 7942 (1991).
  - [7] See for example, Z. Liu and E. Manousakis, *Phys. Rev. B* **45**, 2425 (1992); E. Dagoto, R. Joynt, A. Moreo, S. Bacci, and E. Gagliano, *Phys. Rev. B* **41**, 9049 (1990); D. Poiblanc, T. Ziman, H.J. Schulz, and E. Dagotto, *Phys. Rev. B* **47**, 14267 (1993); G. Martinez and P. Horsch, *Phys. Rev. B* **44**, 317 (1991); P.W. Leung and R.J. Gooding, *Phys. Rev. B* **52**, 15 711 (1995).
  - [8] Some exciton hopping processes, such as  $\tau_x(\mathbf{R}) \rightarrow \tau_x(\mathbf{R} + \hat{y})$ , may disturb the AF spin background. But these integrals are small, at least fourth order in  $t_{pp}$  or  $t_{pd}$ , and their contribution to the exciton dispersion is insignificant.
  - [9] M.J. Rice and Y.R. Wang, *Phys. Rev. B* **36**, 8794 (1987).
  - [10] This is consistent with the local molecular picture. The intra-molecular energies of the exciton states are  $2t_1$  for the  $s$ -wave,  $-2t_1$  for the  $d$ -wave, and zero for the two  $p$ -wave states. This leads to the same conclusion that the S-mode has the highest energy provided  $t_1 > 0$ .
  - [11] There are two nearby peaks in the optical forbidden transitions observed in the EELS in Ref. 3. Here we assume the lower energy state to be the S-mode exciton discussed in the text. A smaller  $t_1$  gives a sharper drop in the intensity of the  $P_1$  mode along [10] direction.
  - [12] P.B. Littlewood, C.M. Varma, S. Schmitt-Rink, and E. Abrahams, *Phys. Rev. B* **39**, 12371 (1989).
  - [13] S.E. Schnatterly, in *Solid State Physics* (academic Press, New York, 1979), vol **34**.
  - [14] Similar to the discussion for the EELS anisotropy in  $\text{BaBiO}_3$ , Y.Y. Wang *et al.*, *Phys. Rev. Lett.* **75**, 2546 (1995).

FIG. 1. Structure of local excitons in insulating Cu-O planes. The open circles represent O-atoms, the solid circles represent Cu-atoms. (a) exciton  $x(\mathbf{R})$ : the quasi-particle is at the vacant Cu-site  $\mathbf{R}$ , and the quasi-hole is on the square of O-atoms with more weight at the left atom and forms a spin singlet with the central Cu-hole at position  $\mathbf{R} + \hat{x}$ . Not shown are a single hole on all other Cu-sites. (b) a simpler representation of (a). (c), excitons  $\bar{x}(\mathbf{R})$ ,  $y(\mathbf{R})$  and  $\bar{y}(\mathbf{R})$ , with the spin singlet at different positions relative to  $\mathbf{R}$ .

FIG. 2. A list of five most important hopping processes from  $x(\mathbf{R})$  to  $\bar{x}(\mathbf{R}')$  and  $y(\mathbf{R}')$ . The other hoppings can be obtained by symmetry. The corresponding effective hopping integrals are given by the Eq. (4).

FIG. 3. Symmetries of the four molecular exciton wavefunctions,  $s$ - and  $d$ -waves in Eq. (7), and the two  $p$ -waves in Eq. (9) with  $k_x = k_y$ . The center  $d$ -wave represents  $\text{Cu}^+$ , a vacancy at Cu-site. The oxygen  $2p_x(2p_y)$  hole wavefunctions are represented by their orbitals. Only charge degrees of freedom are shown. The implicit spins are the same as in Fig. 1.

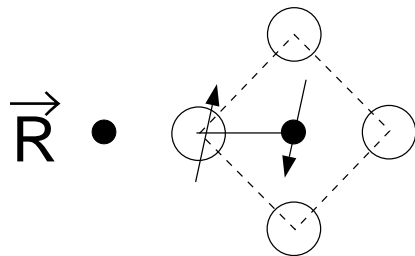
FIG. 4. Calculated exciton energies  $E$  (eV) as a function of  $\mathbf{k} = (k_x, k_y)$ , for the parameters  $t_1 = 0.4$ ,  $t_2 = 0.126$ ,  $t_3 = 0.85$ ,  $t_4 = 0.65$  eV. The energy is measured relative to the  $p_1$ -mode at  $\mathbf{k}=0$ . The thick solid lines show the dispersions along [10] direction. The dispersions of the  $P$ -wave mode are compared very well with the EELS along [10] and [11] dispersions. See Ref. 3 for the detailed comparison.

FIG. 5. Calculated intensities  $I$  (arb. unit) of the exciton transitions as function of  $\mathbf{k}$ , normalized to  $I_0$ . The parameters are as same as those in Fig. 4. The thick solid lines show the intensities along [10] direction. The  $P_2$ -mode is not shown because it is dipole inactive and has no contribution to the intensity for all  $\mathbf{k}$ . The theory is compared well with the EELS along [10] and [11] directions. The intensities for the  $S$ -mode at finite  $\mathbf{k}$  along [10] were observed in the EELS, see Ref. 3.

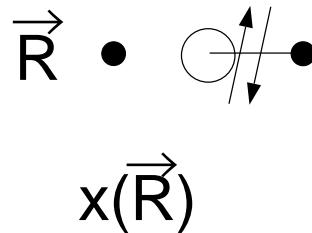
Mode	energy	eigenstate	symmetry at $\mathbf{k} \rightarrow 0$
$P_1$	$-b +  a - \bar{b} $	$(-\eta_-, -1/2, \eta_-, 1/2)$	$p_1$
$P_2$	$b -  a + \bar{b} $	$(-\eta_+, 1/2, -\eta_+, 1/2)$	$p_2$
$S$	$b +  a + \bar{b} $	$(\eta_+, 1/2, \eta_+, 1/2)$	$s$
$D$	$-b -  a - \bar{b} $	$(\eta_-, -1/2, -\eta_-, 1/2)$	$d_{x^2-y^2}$

TABLE I. Solutions of the four exciton modes for  $\mathbf{k}$  along [11] direction. The  $\mathbf{k}$ -dependence in  $a$ ,  $b$  and  $\bar{b}$  is implied, see Eq.(5).  $\eta_{\pm} = \frac{1}{2}(a \pm \bar{b})/|a \pm \bar{b}|$ . The last column applies to the region  $(-b_0 < a_0 < b_0)$  suitable to cuprates, and  $a_0$ ,  $b_0$  are their values at  $k = 0$ .

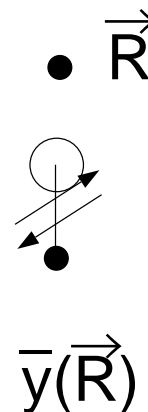
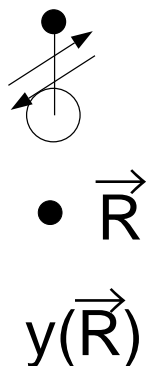
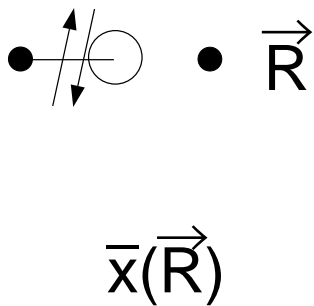
(a)



(b)



(c)



F.C. Zhang

Fig. 1

$$x(\vec{R}) \rightarrow y(\vec{R}) \quad \begin{array}{c} \uparrow \\ \circ \\ \vec{R} \bullet \quad \ominus \nearrow \bullet \end{array} \Rightarrow \begin{array}{c} \bullet \nearrow \\ \circ \\ \bullet \quad \circ \quad \uparrow \end{array} \quad t_{xy}(0)=t_1$$


---

$$x(\vec{R}) \rightarrow y(\vec{R}+\hat{x}) \quad \begin{array}{c} \bullet \\ \downarrow \\ \circ \\ \vec{R} \bullet \quad \ominus \nearrow \bullet \end{array} \Rightarrow \begin{array}{c} \bullet \nearrow \\ \circ \\ \downarrow \quad \circ \quad \bullet \quad \vec{R}+\hat{x} \end{array} \quad t_{xy}(\hat{x})=t_2$$


---

$$x(\vec{R}) \rightarrow y(\vec{R}-\hat{y}) \quad \begin{array}{c} \vec{R} \bullet \quad \ominus \nearrow \bullet \\ \circ \\ \uparrow \bullet \end{array} \Rightarrow \begin{array}{c} \bullet \nearrow \quad \circ \quad \uparrow \bullet \\ \circ \\ \bullet \quad \vec{R}-\hat{y} \end{array} \quad t_{xy}(-\hat{y})=t_2$$


---

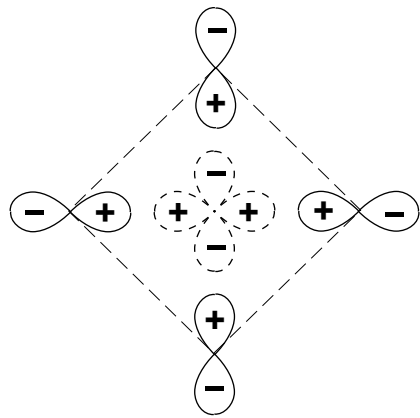
$$x(\vec{R}) \rightarrow \bar{x}(\vec{R}+\hat{x}) \quad \vec{R} \bullet \quad \ominus \nearrow \bullet \Rightarrow \begin{array}{c} \bullet \nearrow \quad \ominus \\ \bullet \\ \vec{R}+\hat{x} \end{array} \quad t_{\bar{x}\bar{x}}(\hat{x})=-t_3$$


---

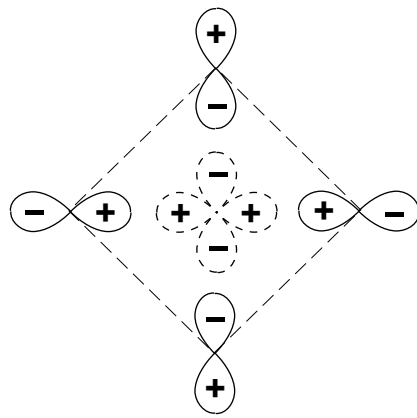
$$x(\vec{R}) \rightarrow \bar{x}(\vec{R}) \quad \begin{array}{c} \uparrow \bullet \quad \circ \quad \bullet \quad \ominus \nearrow \bullet \\ \vec{R} \end{array} \Rightarrow \begin{array}{c} \bullet \nearrow \quad \ominus \quad \bullet \quad \circ \quad \uparrow \bullet \\ \vec{R} \end{array} \quad t_{\bar{x}\bar{x}}(0)=t_4$$

F.C. Zhang

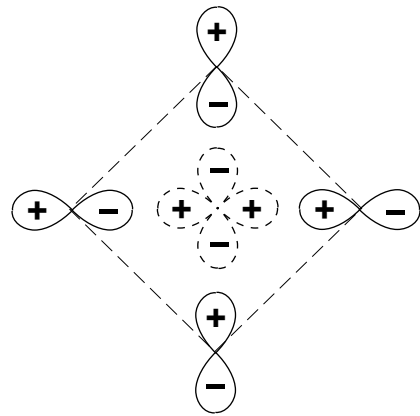
Fig.2



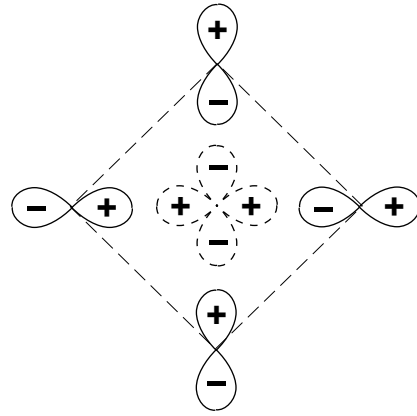
s-wave



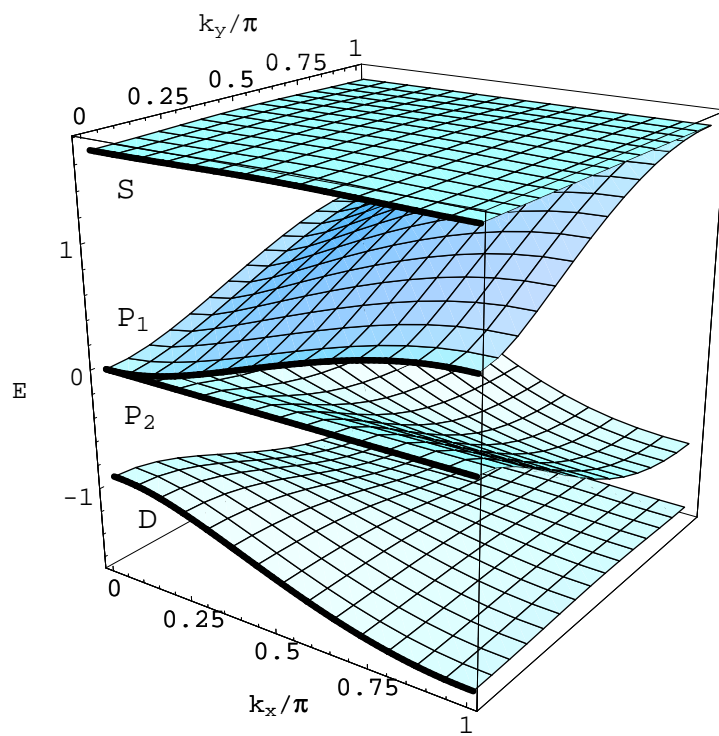
d-wave



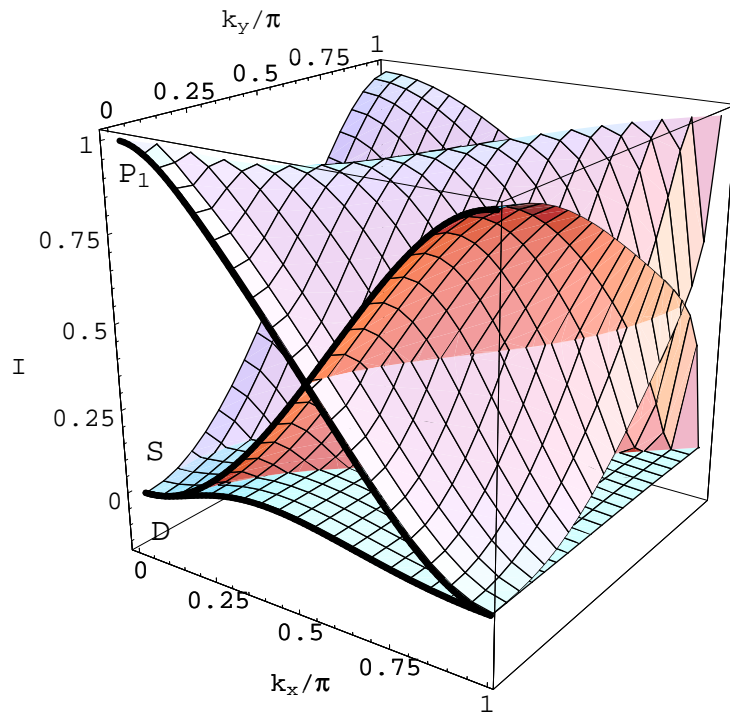
$p_1$ -wave



$p_2$ -wave



F.C. Zhang Fig.4



F.C. Zhang Fig.5